ATLANTIS PRESS
Advances in Engineering Research (AER), volume 174
International Conference on Energy Development and Environmental Protection (EDEP 2018)

Microstructure and Luminescence Properties of Eu^{3+}-doped $BiPO_4$ Phosphors by Hydrothermal Synthesis Method

Shu-Qing YAN, Shan-Shan MA, Cong-Guo LONG and Rui ZHENG

School of Mathematics and Statistics, North China University of Water Resources and Electric Power; Zhengzhou, 450011, China

E-mail: yanshuqing1979@163.com

Keywords: Luminescence property, Dosage, Eu^{3+} ions, Hydrothermal method.

Abstract. In this paper, the hydrothermal method was used to synthesis the Eu^{3+} ions activated BiPO4 powders. The characteristic of the $BiPO_4$:xEu^{3+} samples were analyzed with different testing methods. XRD results show that Eu^{3+}-doped $BiPO_4$ samples presented a hexagonal structure, and with the increasing of Eu^{3+} concentration, angle of diffraction peaks becomes larger. The SEM images show that the Eu^{3+}-doped $BiPO_4$ powders are rod like crystals and it was estimated that the sub micrometer sizes were between 0.1-0.15μm. The best excitation wavelength was 395nm. The fluorescence emission spectra of $BiPO_4$:xEu^{3+} samples showed that the bands of different positions have associated with the $^5D_0 \rightarrow {}^7F_J$ electronic transitions characteristics of the Eu^{3+} ions. The intensity of emission spectra increases to the highest as the dosage concentration of Eu^{3+} ions up to 0.05mol.

Introduction

Due to the multifarious applications as catalyst, co precipitation, separation of radioactive elements, and so on, $BiPO_4$ has been widely known as a type of metal phosphate [1]. Not long ago, $BiPO_4$ has been found that it can emit light around 437nm upon UV-excitation. Great attention has been paid on the luminescence properties of $BiPO_4$ material in the luminescence field [2-3]. Because the ionic radius of Bi^{3+} is close to those of rare earth ions, rare earth ion can be successfully doped into $BiPO_4$ materials. At the same time, rare-earth based optical materials exhibit excellent physics and chemical properties [4], especially of trivalent europium (Eu^{3+}) ions. It has been recognized as an efficient red luminescent phosphor due to its $^5D_0 \rightarrow {}^7F_j$ (j=0, 1, 2, 3, 4) transitions [5–7]. Therefore, Eu^{3+} ions can be doped in $BiPO_4$ due to the similar ionic size and the same oxidation states of Eu^{3+} and Bi^{3+}. Sun et al. has synthesized the polyhedrons $BiPO_4$:xEu^{3+} structure successfully, and studied its luminescence properties [4]. However, the particle sizes of $BiPO_4$:xEu^{3+} powders is large by a solid state reaction method. Ultrafine nanoparticles have larger surface area than the bulk materials, which is very useful for good luminescent properties. Hydrothermal synthesis is a good method for preparing nanometer particles [8-9]. It is also used to obtain some metastable polymorphs that are usually not available through traditional solid state reaction. In the present studies, the hydrothermal synthesis method was used and the $BiPO_4$:xEu^{3+} powders were synthesis by a facile hydrothermal route. The effect of different Eu^{3+} ions on the microstructure and luminescence properties was studied carefully.

Experimental

Preparation

High purity reagents of Bi_2O_3, Eu_2O_3 and $NH_4H_2PO_4$ were used to prepare the Eu ions doped $BiPO_4$ samples without further purification. The samples are $BiPO_4$:xEu^{3+} powder and the x design is 0.01, 0.03, 0.05 and 0.07mol. Firstly, stoichiometric amounts of Bi_2O_3 and Eu_2O_3 were dissolved in dilute HNO_3 solution under stiring for obtaining 2.5mmol of Bi $(NO_3)_3$ and 2.5x mmol of Eu$(NO_3)_3$ aqueous solutions. Meanwhile, 2.5mmol of $NH_4H_2PO_4$ was dissolved into 15mL of deionized water. Then the $NH_4H_2PO_4$ solution was dropped into the Bi $(NO_3)_3$ and Eu$(NO_3)_3$ solution under

electromagnetic stirring, until the white $BiPO_4$: xEu^{3+} powder was obtained. After 30min of an additional electromagnetic stirring, the final suspension was transferred into a 50mL high pressure reactor. The reactor was sealed and maintained at 120°C for 5h. The reactor is then cooled down to room temperature, the $BiPO_4$:xEu^{3+} powders were collected, washed with deionized water and dried at 80°C for 8h.

Characterization

The powder X-ray diffraction (XRD) with an X-ray diffract meter (model D/max-γA, Rigaku, Japan) using graphite monochromatized Cu Kα irradiation (λ = 0.15406 nm) was used to examine the crystallinity and phase purity of the samples. The acceleration voltage was 40 kV and the current was 44 mA. A FEI-Quanta 200 scanning electron microscope was used to observe the microstructures of the test samples. A Hitachi 650 spectrophotometer equipped with a 150w xenon lamp as the excitation source was used to test the excitation and emission spectra. It's important to note that all the measurements were carried out at room temperature.

Results

Fig.1 shows the XRD test results of as-prepared $BiPO_4$:xEu^{3+} (x=0, 0.01, 0.03, 0.05, and 0.07) samples. All diffraction peaks can be well indexed to the hexagonal structure of $BiPO_4$ with JCPDS no.45-1370. It also shows that no impurity peaks are observed in these patterns. This indicates that the addition of Eu^{3+} do not change on the formation of the samples and introduce any impurity phases. XRD results also show that the crystallization of $BiPO_4$: xEu^{3+} samples is better than that of $BiPO_4$ sample due to the sharp diffraction peaks. However, the position of the diffraction peaks shift slightly toward higher angle side with the increasing Eu^{3+} content. This indicates that the lattice parameters are slightly decreased with the increase of Eu^{3+} content, and it can be attributed to the smaller radius of Eu^{3+}(0.095nm) than that of Bi^{3+}(0.103nm). The dopant ions of Eu^{3+} are well incorporated into the lattice sites of Bi^{3+}, which leads to the decrease in inter atomic distance [10]. However, the shift quantity of the diffraction peaks' position is not further increasing with the increase of Eu^{3+} ions. This might be something to do with the doping amount and doping location of Eu^{3+} ions. Fig.2 shows the crystal structure of $BiPO_4$ and the digits 1-5 represents the location of five adjacent Bi^{3+} ions. The spacing results of two adjacent Bi ions are 0.408nm, 0.283nm, 0.699nm, 0.486nm, 0.192nm, 0.193nm and 0.571nm for 1→2 (the spacing from Bi1 to Bi2), 1→4, 2→3, 2→4, 2→5, 3→4 and 3→5, respectively. This indicating that the different sites the Eu^{3+} ions incorporated into the lattice sites of Bi^{3+} while lead to the different degree of decrease in inter atomic distance.

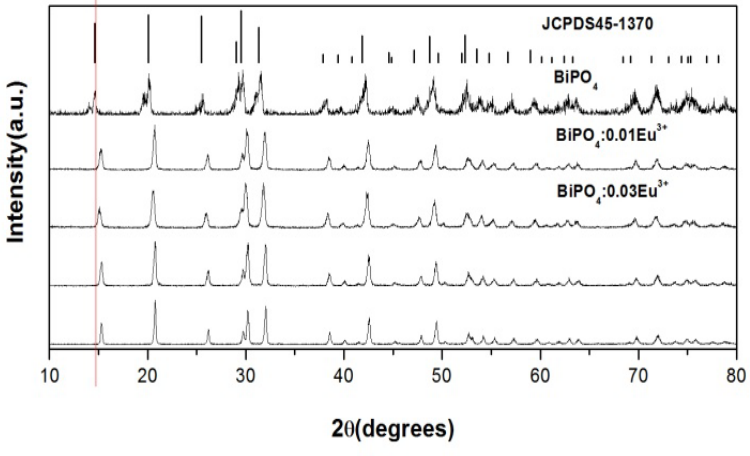

Fig. 1 XRD patterns of $BiPO_4$:xEu^{3+} samples.

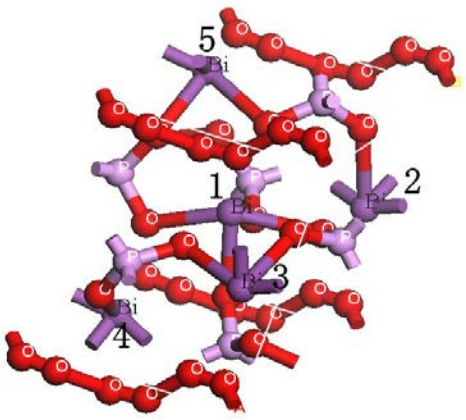

Fig. 2 Crystal structure of BiPO4.

From the analysis of XRD, it was evident that well-crystallized $BiPO_4$:xEu^{3+} samples can be

obtained by hydrothermal synthesis method. The dosage of Eu^{3+} has no significant influence on the phase and crystal structure of $BiPO_4$, only the lattice parameters have some degree of modification. It is due to the different ionic radius of Eu^{3+} and Bi^{3+}.

Average grain size of the test samples can be estimated according to Scherrer equation [11],

$$D = k\lambda / (\beta \cos\theta) \tag{1}$$

All major reflection peaks ((100), (101), (110), (200), (102) and (211)) were chosen to estimate the average crystallite size. The calculated average crystalline sizes through Scherrer equation are about 31nm, 31nm, 28nm, 35nm and 46nm for $BiPO_4$, $BiPO_4$:$0.01Eu^{3+}$, $BiPO_4$:$0.03Eu^{3+}$, $BiPO_4$:$0.05Eu^{3+}$ and $BiPO_4$:$0.07Eu^{3+}$, respectively.

Fig.3 shows the SEM image of $BiPO_4$ and $BiPO_4$: $0.05Eu^{3+}$ samples. The microstructures show that the $BiPO_4$ white sample powders are rodlike crystals with submicrometer sizes in the range of 0.1-0.2μm. The size is greatly different from the estimated results from Scherrer equation. It can be attributed to the rodlike crystal morphology, which is great different from the circular particles. However, the sizes and morphologies have no changes by comparison the SEM image of $BiPO_4$ and $BiPO_4$:$0.05Eu^{3+}$ sample. More telling, it has no influences on the sizes and morphologies of $BiPO_4$ samples at the current doping concentration of Eu^{3+} ions.

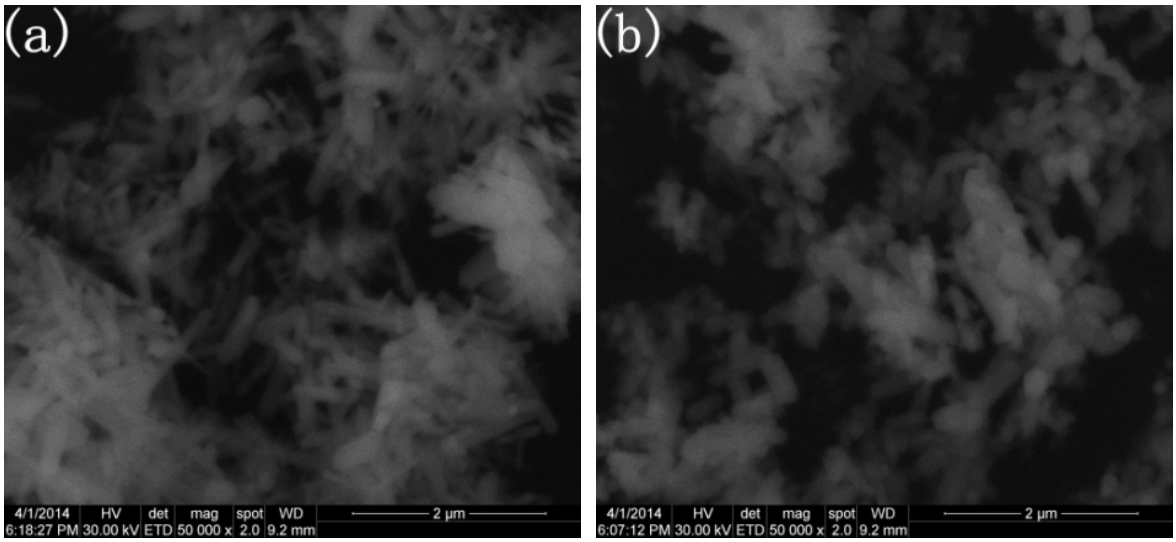

Fig. 3 SEM image of (a) $BiPO_4$ and (b) $BiPO_4$: $0.05Eu^{3+}$ sample.

Emission spectra of $BiPO_4$:$0.05Eu^{3+}$ sample was tested as shown in Fig.4. It shows a broad excitation band in the wavelength range 300-500nm. The reason can be attributed to the intra-configurational (f-f) transitions of Eu^{3+} at the hexagonal Bi^{3+} site of $BiPO_4$ crystal. The strongest sharp excitation line located at 395 nm and it is assigned to $^7F_0 \rightarrow {}^5L_6$ transition of Eu^{3+}. This indicates the interaction is stronger between O^{2-} and Eu^{3+}[12]. Other weak excitation lines can be attributed to $^7F_0 \rightarrow {}^5D_4$ (365 nm), $^7F_0 \rightarrow {}^5L_7$ (380 nm), $^7F_0 \rightarrow {}^5D_3$ (419 nm), and $^7F_0 \rightarrow {}^5D_2$ (468 nm), respectively. The test results show that the Eu^{3+}-doped $BiPO_4$ phosphor can be effectively excited by radiations of wavelength in the near-UV region, therefore it is useful in white LEDs.

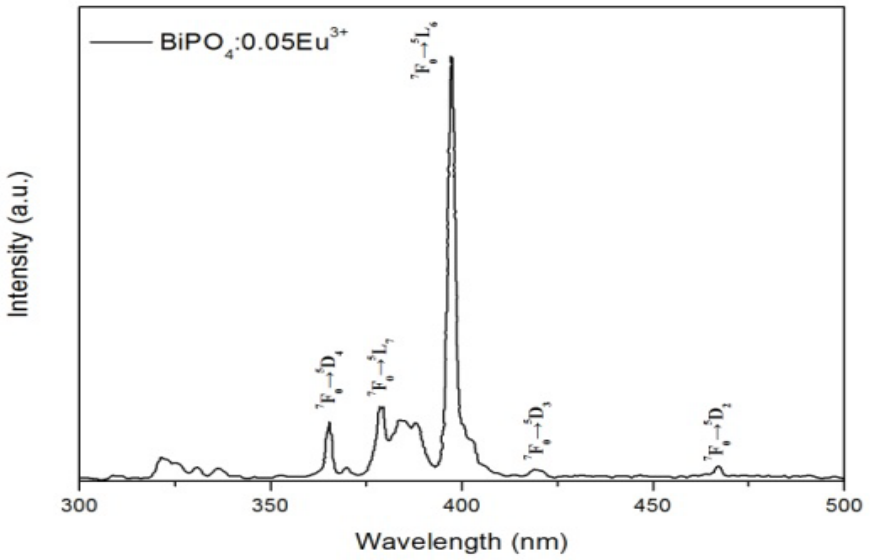

Fig. 4 Excitation spectra of $BiPO_4$: $0.05Eu^{3+}$ sample.

Fig.5 shows the emission spectra of $BiPO_4$:xEu^{3+} samples. The emission spectra were measured in the range of 500-750nm at room temperature. It can be seen that the emission spectrum lines of the test samples locate mainly in the red area at 395 nm. The most intense peak is at 594nm and carries a relatively weak peak at 587 nm. It can be attributed to $^5D_0 \rightarrow ^7F_1$ transitions. The other bands can be assigned as $^5D_0 \rightarrow ^7F_2$ at 614 and 618nm, $^5D_0 \rightarrow ^7F_3$ at 652nm, and $^5D_0 \rightarrow ^7F_4$ at 688 and 698nm, respectively. These lines are all come from the $4f^6$ configuration of Eu^{3+} ions and the transitions is from its excited $^5D_0$ level to ^7F_J (J=0–4) ground level. As well known, the $^5D_0 \rightarrow ^7F_1$ magnetic dipole transition in the inversion symmetry site, while the $^5D_0 \rightarrow ^7F_2$ transition contains a noninversion symmetry [13-15]. Fig.4 shows that the intensity of $^5D_0 \rightarrow ^7F_1$ magnetic dipole transition is dominant over the $^5D_0 \rightarrow ^7F_2$ electric dipole transition. It suggests that a higher occupancy of Eu^{3+} ions in a crystallographic symmetric environment.

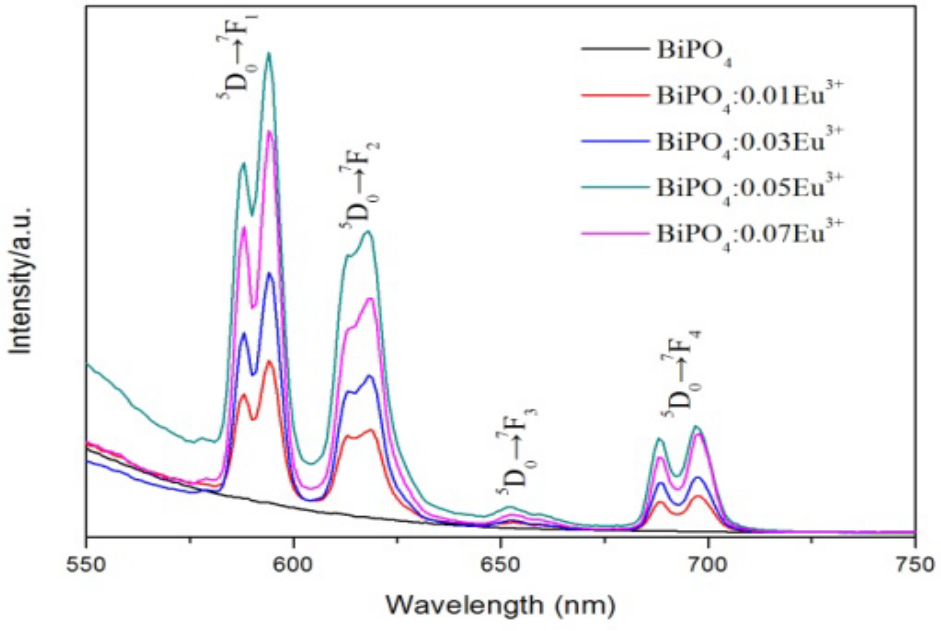

Fig. 5 Emission spectra of BiPO4:xEu^{3+} samples.

The emission intensity increases with increasing the concentration of Eu^{3+} ions until the concentration of Eu^{3+} ions reaches to 0.05mol and then decreases. Analysis suggests that the number of luminescence centers increases with an increase in doping concentration firstly. As a result the emission intensity increases. However, the distance of Eu^{3+} ion and Eu^{3+} ion decreases with the increasing of Eu^{3+} dosage concentration, especially as the doping concentration of Eu^{3+} exceeds 0.05mol. The interaction of Eu^{3+} ions in the excited states is enhanced, and one of the two Eu^{3+} ions is forced to release energy and returns to ground state through non-radiative transition, the other one is inspired to a highly excited state at the same time. This leads to the decrease of luminescent transition probability [16]. In short, the excess of Eu^{3+} in the host has a clear concentration quenching which leads to the spectral intensity is decreased obviously as shown in Fig.4.

Discussion

$BiPO_4$:Eu^{3+} (0.01-0.07mol) nanophosphors were prepared by a hydrothermal synthesis method. The nanorods were formed with diameter of 0.1-0.2μm and length of 0.3-0.7μm. XRD pattern indicates that Eu^{3+} ions are incorporated into the lattice sites of Bi^{3+} and lead to distort of the hexagonal structure. The reason can be attributed to the Eu^{3+} (0.095nm) ion has a smaller radius than that of Bi^{3+} (0.103nm). The improved luminescence property can be attributed to the Eu^{3+} ions dope into the host and occupy the lattice sites of Bi^{3+}. The electrons transfer from the filled molecular orbital of oxygen to the partially-filled 4f shells of Eu^{3+} ions, which led to a wider charge transfer band formed on the spectrum. A strong mixture of charge transfer states leads to a high increase in luminescence property. However, Bi^{3+} ions can only accommodate small percentage of impurity ions for optimum strain relief and charge imbalance. Eu^{3+} ions are possible reside on the surface or grain boundaries of $BiPO_4$ nanocrystals, and the distance between Eu^{3+} ions decreases with the increasing Eu^{3+} ions concentration. This leads to the probability of energy transfer between two activator Eu^{3+} ions is higher. It has a clear concentration quenching due to the non-radiative energy transfer among luminescent centers and then the PL intensity decreases[12]. The test results show that the concentration quenching of Eu^{3+} dosage concentration in $BiPO_4$ is 5mol%.

Conclusions

The Eu^{3+} ions activated $BiPO_4$ powders were synthesized by a hydrothermal method. The XRD, SEM and luminescence spectroscopy were used to analyze the effect of Eu^{3+} contents on the luminescence properties of BiPO4 powder. The conclusions are as following:

(1) The $BiPO_4$:xEu^{3+} samples presented a hexagonal structure, the phase structures and morphologies have not changed after doping Eu^{3+} ions.

(2) The doped Eu^{3+} ions replaces the lattice sites of Bi^{3+} as a result the atomic distance decreases. The XRD results also approved it.

(3) The best excitation wavelength of 395nm was chosen, and the emission spectrum mainly located in the red area.

(4) The emission spectra show that the bands of different positions relate to the $^5D_0 \rightarrow {}^7F_J$ electronic transitions characteristics of the Eu^{3+} ions. The dosage content of Eu^{3+} has a remarkable impact on emission properties. The intensities of emission spectra increase as increasing dosage content of Eu^{3+} ions until up to 0.05mol and then decreases.

Acknowledgments

This work is financially supported by the Science and technology research project of Henan, China (grants no. 162102210079).

Reference

[1] Zhong jianming, Zhao weiren, Lan licai, ect, J. Rare Earth, .32(1):5-11(2014).

[2] A. Wolfert, E.W. J. L. Oomen, G. Blasse, J. Solid State Chem. **59**, 280 (1985).

[3] F. Xue, H. Li, Y. Zhu, S. Xiong, X. Zhang, T. Wang, X. Liang, Y. Qian, J. Solid State Chem. 182, 1396 (2009).

[4] Xiaoyu Sun, Xiaodan Sun, Jian He, ect, ceramics international, 2014,40:7647-7650

[5] H. Shabir, B. Lal, M. Rafat, J. Sol-Gel Sci Tech. 53(2010)399-404.

[6] P. Zhang, Y. Wang, Y. Wen, D. Wang, Y.Tao, Opt Mater, 33(2011)475-479.

[7] G. Phaomei, W.R. Singh, R.S. Ningthoujam, J.Lumin, 131(2011)1154-1171

[8] C. Cao, A. Xia, S. Liu, L. Tong, J. Mater. Sci: Mater. EL. **24**, 4901 (2013).

[9] L. Miao, H. Zhang, Y. Zhu, Y. Yang, Q. Li, J. Li, J. Mater. Sci: Mater. EL. **23**, 1887 (2012).

[10] L. F. Koao a, F.B.Dejene a,n, R.E.Kroon b, H.C.Swart, J. LUMIN. 147, 85–89(2014)

[11] B.D. Cullity, Elements of X-ray Diffraction, second edn. (Addison-Wesley Publishing Company, London, (1978), pp. 101–102.

[12] M. Shivram, S.C. Prashantha, H. Nagabhushana, et al, Spectrochim Acta A, 120(2014)395-400

[13] B.F. Lei, S.Q. Man, Y.L. Liu, S. Yue, Mater. Chem. Phys. 124, 912 (2010).

[14] B.R. Judd, Phys. Rev. 127(1962)750-761.

[15] W. Li, J. Lee, J.Phys.Chem.C 112(2008)11679-11684.

[16] G. Ju, Y. Hu, H. Wu, Z. Yang, C. Fu, Z. Mu, F. Kang, Opt. Mater. 33 (2011) 1297-1301.